Enhancement of collagen 1 expression by prostaglandin F2α agonists is pivotally involved in the pathogenesis of deepening of the upper eyelid sulcus

Kaku Itoh[1], Yosuke Ida[1], Hiroshi Ohguro[1], and Fumihito Hikage[1]

[1]Sapporo Medical University

August 25, 2020

Abstract

Background and Purpose:Deepening of the upper eyelid sulcus (DUES) is recognized as an unfavorable and causeless side effect observed among long-term users of prostaglandin analogues (PGs). To elucidate the molecular pathology of DUES, we characterized thee-dimension (3D) cultures of human orbital fibroblasts (HOFs). Experimental Approach: HOF organoids were cultured without or with their adipogenic differentiation and at several concentrations (1, 100, 10000 nM) of PGs (bimatoprost acid; BIM-A, PGF2α, latanoprost acid; LAT-A). Their sizes, the mRNA expression of adipogenic related genes, extracellular matrix (ECM) and tissue inhibitors of metalloproteinases (TIMPs) were measured by electron microscope (EM) and the physical properties were measured by a micro-squeezer. Key Results: Adipogenesis caused significant downsizing of the organoids, and these were markedly inhibited in the presence of PGs in a concentration dependent manner. BIM-A was the most effective. The downsizing induced by PGs was also observed in conditions without adipogenesis. The size of each organoid under several conditions was inversely correlated with the mRNA expression profile of collagen 1 (COL1), which was also confirmed by immunolabeling. An mRNA expression profile similar to that for COL1 was also observed in Lysyl oxidase (LOX) and TIMP2. Analyses by EM and the micro squeezer clearly indicated that PGs induced an increase in ECM deposits and the physical solidity of the organoids. Conclusions and Implications: The findings reported herein indicate that PGs affects the expression of LOX, COL1 and TIMP2 which, in turn, modulate the 3D ECM network within the organoids, thus resulting in their downsizing.

Ενηανσεμεντ οφ σολλαγεν 1 εξπρεσσιον βψ προσταγλανδιν Φ2α αγονιστς ις πιοταλλψ ινολεδ ιν τηε πατηογενεσις οφ δεεπενινγ οφ τηε υππερ εψελιδ συλςυς

Authors

Kaku Itoh, Yosuke Ida, Hiroshi Ohguro, Fumihito Hikage.

Departments of Ophthalmology, Sapporo Medical University School of Medicine

Short title: DUES model of 3D culture

Key words: deepening of the upper eyelid sulcus (DUES), prostaglandin (PG) analogues, 3-dimension (3D) tissue culture

All correspondence should be addressed to Fumihito Hikage

Tel# 81-11-611-2111, Fax# 81-11-613-6575, e-mail:*fuhika@gmail.com*

Both authors (K. I and Y. I.) contributed equally to this study.

Background and Purpose: Deepening of the upper eyelid sulcus (DUES) is recognized as an unfavorable and causeless side effect observed among long-term users of prostaglandin analogues (PGs). To elucidate the

molecular pathology of DUES, we characterized thee-dimension (3D) cultures of human orbital fibroblasts (HOFs).

Experimental Approach: HOF organoids were cultured without or with their adipogenic differentiation and at several concentrations (1, 100, 10000 nM) of PGs (bimatoprost acid; BIM-A, PGF2α, latanoprost acid; LAT-A). Their sizes, the mRNA expression of adipogenic related genes, extracellular matrix (ECM) and tissue inhibitors of metalloproteinases (TIMPs) were measured by electron microscope (EM) and the physical properties were measured by a micro-squeezer.

Key Results: Adipogenesis caused significant downsizing of the organoids, and these were markedly inhibited in the presence of PGs in a concentration dependent manner. BIM-A was the most effective. The downsizing induced by PGs was also observed in conditions without adipogenesis. The size of each organoid under several conditions was inversely correlated with the mRNA expression profile of *collagen 1 (COL1)* , which was also confirmed by immunolabeling. An mRNA expression profile similar to that for *COL1* was also observed in*Lysyl oxidase (LOX)* and *TIMP2* . Analyses by EM and the micro squeezer clearly indicated that PGs induced an increase in ECM deposits and the physical solidity of the organoids.

Conclusions and Implications: The findings reported herein indicate that PGs affects the expression of *LOX, COL1* and*TIMP2* which, in turn, modulate the 3D ECM network within the organoids, thus resulting in their downsizing.

1—INTRODUCTION

Prostaglandin analogues (PGs) are typically used as first-line drugs because of their efficiency in lowering elevated intraocular pressure (IOP) through their FP receptor as well as not having any serious systemic side effects (2017; Alm, 2014; Ota, Aihara, Narumiya & Araie, 2005). It should be noted in this respect that, among long-term users of PGs, local side effects called "prostaglandin-associated periorbitopathy (PAP)" including conjunctival injection, hyperpigmentation of the iris and skin, elongation of the eyelashes, and deepening of the upper eyelid sulcus (DUES) have recently been reported (Alm, Grierson & Shields, 2008; Nakakura et al., 2014; Shah et al., 2013). Among these, DUES is a cosmetically non-negligible side effect, and has been reported in most PGs including bimatoprost (BIM), travoprost, tafluprost, and latanoprost (LAT) (Aihara, Shirato & Sakata, 2011; Maruyama, Tsuchisaka, Sakamoto, Shirato & Goto, 2013; Peplinski & Albiani Smith, 2004; Sakata, Shirato, Miyata & Aihara, 2014). As possible mechanisms responsible for causing DUES, orbital fat atrophy, as observed by MRI and histological analysis appears to be primarily involved (Jayaprakasam & Ghazi-Nouri, 2010). However, their precise molecular etiology remains to be elucidated.

Adipocytes are involved in a variety of physiological functions of fat storage and the mobilization of free fatty acids in response to a variety of nutritional and hormonal conditions (Kershaw & Flier, 2004). During their adipogenic differentiation, preadipocytes grow into mature form of adipocytes and this process is minutely regulated by several adipogenesis-related genes such as $PPAR\gamma$ (Evans, Barish & Wang, 2004; Gregoire, Smas & Sul, 1998). Several previous reports revealed that PGs suppress adipogenesis through activation of the FP receptor (Taketani, Yamagishi, Fujishiro, Igarashi, Sakata & Aihara, 2014). Thus, such PG induced suppression of the adipogenic differentiation of the adipocytes may primarily be involved in the pathogenesis causing DUES.

In our precedent study, to establish a DUES model by PGs, a three-dimension (3D) tissue culture was employed using 3T3-L1 cells, the most common preadipocyte cell line, and 3D organoids were obtained (Ida, Hikage, Itoh, Ida & Ohguro, 2020). Upon adipogenesis, the organoid size, and lipid and extracellular matrices (ECMs) content increased dramatically, and such increases were significantly inhibited in the presence of PGs. We therefore concluded that a 3D tissue culture may suitably replicate DUES pathology and therefore should be useful for developing an understanding of the disease etiology of DUES. Since it was suggested that the physiological properties of human orbital fatty tissues may be different with those of 3T3-L1 cells (Mori, Kiuchi, Ouchi, Hase & Murase, 2014), human orbital fibroblasts (HOFs) rather than 3T3-L1 cells would be desirable as a model mimic DUES etiology. In our subsequent pilot study, although we also found similar

effects of PGs toward 3D HOF organoids, the of effect of PGs on lipid metabolisms during their adipogenesis was much less as compared to the 3D organoid of 3T3-L1 cells (Itoh, Hikage, Ida & Ohguro, 2020). This evidence prompted us to speculate that FP agonists may affect mechanisms other than adipogenesis in 3D HOF organoids.

In the current study, to further characterize a DUES model by 3D culture using HOFs, we examine the concentration dependency among PGs, the influence of PGs toward adipogenesis and ECM expression, as well as their efficacy on the structural and physical properties of the 3D HOFs organoids.

2—METHODS

2.1 | Two-dimension (2D) and three-dimension (3D) Cultures of human orbital fibroblasts (HOFs) and their adipogenic differentiation in the presence or absence of PGs

This study, which was performed at the Sapporo Medical University Hospital, Japan, was approved by the institutional review board (approved number, 312-3190) and according to the tenets of the Declaration of Helsinki as well as national laws for the protection of personal data. Informed consent was obtained from all participants in this study.

Orbital fat explants from 4 patients with orbital fat herniation were cultured in a 2D grown medium (DMEM supplemented with 10% FBS, 1% L-Glutamine, and 1% Antibiotic-Antimycotic) on 100 mm dishes at 37°C with 5 % CO_2 in which the medium was changed every other day. After the initial culture, the HOFs were obtained during 3 to 7 passages and further cultured, as described above until they reached 100% confluence. For the induction of adipogenic differentiation of the 2D cultured HOFs, overconfluent 2D cells were obtained by further culturing for 2 days, and thereafter cultured according to the adipogenesis induction protocol; supplementation of the culture medium with an adipogenesis cocktail (250 nM dexamethasone, 10 nM T3, 10 μg/ml insulin, and 10 mM troglitazone) during Day 1-5, and with the dexamethasone-free adipogenesis cocktail during Day 6-12.

For 3D organoid cultures, 100% confluent 2D cultured HOFs obtained as above were washed twice with PBS, resuspended in 2D grown medium, and centrifuged at 300 x g for 5 mins. HOF pellets were collected and resuspended in 3D organoid medium (2D grown medium supplemented with 0.25% Methocel to stabilize 3D organoid). A 28μL portion of the suspension containing approximately 20,000 HOFs cells was cultured in each well of a hanging drop culture plate (No. HDP1385; Sigma-Aldrich) until Day 12. During the 3D culture, half of the medium was exchanged daily with fresh medium. Adipogenic differentiation of the 3D HOFs culture was induced following the induction protocol described above. Alternatively, as experimental conditions without adipogenesis, 2D HOFs cells or 3D HOFs organoids were assessed as above in the medium used above, supplemented with 0.1% DMSO during the entire 12 days culture period. For the evaluation of drug efficacy of the PGs toward 3D HOFs organoids, different concentrations of bimatoprost acid (BIM-A), PGF2α or latanoprost acid (LAT-A) were added during Day 1 through 12. These 2D HOFs cells and 3D HOFs organoids were each collected at Day 12 and used for the analytical studies described below.

2.2 | Characterization of 3D organoid configuration and measurement of the mean sizes of the 3D HOFs organoids

The 3D organoid configuration was observed by phase contrast (PC, Nikon ECLIPSE TS2; Tokyo, Japan) and scanning electron microscopy (EM, HITACHI S-4300; Tokyo, Japan) as described previously. For measurement of each 3D organoid size, the largest cross-sectional area (CSA) of the PC image was measured and analyzed using the Image-J software version 1.51n (National Institutes of Health, Bethesda, MD).

2.3 | Lipid staining by BODIPY of 2D HOFs cells or 3D HOFs organoids

2D HOF cells or 3D organoids obtained at Day 12 as above were washed with PBS and then fixed in 4% paraformaldehyde (PFA) in PBS for 10 min at room temperature (RT). These organoids were incubated in 0.2% 1:1000 dilutions of BODIPY (488 nm), DAPI and phalloidin (594 nm) in PBS for 1-3 hrs. Fluorescence

intensity of the BODIPY-stained lipid droplets was measured using a Nikon A1 confocal microscope (Tokyo, Japan) and quantified using the Image J software version 2.0.0 (NIH, Bethesda, MD).

2.4 | Gene expression analysis

Total RNA was extracted from 16 of the 3D HOFs organoids using a RNeasy mini kit (Qiagen, Valencia, CA). Reverse transcription was assessed with the SuperScript IV kit (Invitrogen) as according to the manufacturer's protocol. Respective gene expression was quantified by real-time PCR with either Power SYBR Green or Universal TaqMan Master Mix using a StepOnePlus machine (Applied Biosystems/Thermo Fisher Scientific). After normalization by the expression of the housekeeping gene 36B4 (RPLP0), each cDNA quantities are shown as fold change relative to the control. DNA sequences of primers and TaqMan probes are shown in Table 1.

2.5 | Immunocytochemistry of 3D HOFs organoids

Immunocytochemistry of the 3D HOFs organoids was conducted by a recently described method. All procedures were performed at RT unless otherwise stated. Briefly, the 3D HOF organoids obtained at Day 12 as above were fixed overnight in 4% PFA in PBS, blocked in 3% BSA in PBS for 3 hrs, washed twice with PBS for 20 mins, and incubated overnight with an anti-human COL1 rabbit antibody (1:200 dilutions) at 4°C. After washing 3 times with PBS for 1 hr, the specimens were incubated with 1000 times diluted goat anti-rabbit IgG (488 nm), phalloidin (594 nm) and DAPI for 3 hrs. a cover glass was then mounted with ProLong Gold Antifade Mountant, and their immunofluorescent images (serial-axis 2.2-μm interval images during a z-plane between 35-μm from their surface) were obtained using a ×20 air objective with a resolution of 1024 × 1024 pixels (Nikon A1 confocal microscopy). For analysis of their signal intensity, the maximum intensity/surface area among above the z-plane areas was calculated using Image J (NIS-Elements 4.0 software) as follows: surface area=$D \times A/(A+\pi \times H^2)$, where D (μm) indicates the organoid diameter, A (μm^2) indicates the area of the sectioned organoid, and H (μm) indicates height (=35-μm).

2.6 | Physical properties of 3D HOFs organoids

To examine the physical properties of the 3D HOF organoids, their micro indentation force was measured using a micro-squeezer (MicroSquisher, CellScale, Waterloo, ON, Canada) as described previously (Yu, Kornmuller, Brown, Hoare & Flynn, 2017). The force required (force/displacement, μN/μm) to compress a single 3D HOF organoid until a 50 % deformity was reached during 20 seconds was measured.

2.7 | Statistical analysis

All statistical analyses were assessed using GraphPad Prism 7 (GraphPad Software, San Diego, CA). A one-way ANOVA was used, followed by a Tukey's multiple comparison test for evaluation of the difference among matched multiple group comparisons. Data are presented as arithmetic means ± SEM.

3 | RESULTS

3.1 | Comparison between 2D and 3D cell cultures of HOFs under adipogenic differentiation (DIF+)

In our preceding study, to elucidate the molecular etiology of DUES by PGs, we replicated an *ex vivo* model of DUSE using a 3D culture of 3T3-L1 cells or HOFs, and found that either 100 nM BIM-A or 100 nM PGF2α induced a significant suppression in HOF organoid maturation presumably by modulation of their adipogenesis and /or ECM expressions (Ida, Hikage, Itoh, Ida & Ohguro, 2020; Itoh, Hikage, Ida & Ohguro, 2020). In this study, to investigate the pharmacokinetics of PGs in the case of the DUES model further, the concentration dependency among PGs, to influence adipogenesis, and their efficacy on structural and physical properties of the 3D organoids was examined. Before these analyses, in order to confirm that our 3D organoid culture was actually suitable for this research purpose, adipogenesis of the HOFs was compared between our 3D culture and conventional 2D culture methods. As shown in Fig. 1 (Panel A), our HOF 3D culture could reproduce the formation of uniform round-shaped spheroidal organoids from 20,000 HOFs cells that were gradually growing smaller by Day 12 of their maturation, and a significant enlargement

upon adipogenic differentiation (DIF+) compared to 3D HOFs preadipocytes (DIF-) was found. Similar to the adipogenesis, lipid staining with BODIPY (Panel B), and the expression of the*ΠΠΑΡγ* (Panel C) were significantly enhanced. While in contrast, in the 2D culture, positive BODIPY staining was negligible and only a faint staining spot was detected by chance even though the induction of adipogenic differentiation was identical with that for a 3D culture (Panel B). In addition, the extent of adipogenesis-induced enhancement of the expression of the *ΠΠΑΡγ* in 2D HOFs cells was much less as compared to that in 3D HOF organoids (Panel C). These observations indicate that the adipogenesis of HOFs was more potently induced in our 3D organoid culture as compared to the conventional 2D culture. We therefore conclude that our 3D HOF organoid culture should be suitable for use in our current investigation.

3.2 | Effects of different concentrations of PGs on the sizes of the 3D HOFs organoids under adipogenic differentiation (DIF+)

As shown in Fig. 2, the DIF+ induced enlargement of the HOF organoid sizes was significantly suppressed in the presence of BIM-A, PGF2α or LAT-A in a concentration dependent manner (1, 100 or 10000 nM). Among these PGs, BIM-A showed the most potent effects, and the effects of PGF2α and LAT-A were similar. Thus, a subsequent analysis was conducted by using 100 nM BIM-A and 100 nM PGF2α. These differences in drug efficacy among PGs is in agreement with clinical observations that BIM most frequently causes DUES, as evidenced by many published reports, suggesting that our 3D culture HOFs well replicated the pathogenesis of DUES.

3.3 | Effects of PGs on the sizes of the 3D HOFs organoids preadipocytes (DIF-)

To elucidate whether these PG-induced effects toward the 3D HOF organoids as above was dependent on their adipogenesis or not, the effects of PGs toward the 3D HOF preadipocyte organoids (DIF-) were also examined. As shown in Fig 3, the downsizing effects toward the DIF- 3D organoids by both 100 nM BIM-A and 100 nM PGF2α were still observed after Day 2 during the 3D culture, although these effects were much less than those with adipogenesis, as describe in Fig. 2. Taken together, downsizing effects of the 3D HOFs organoids by PGs occurred during the maturation of the 3D HOF preadipocyte organoids themselves and those effects were markedly enhanced upon their adipogenesis.

3.4 | Comparison between 3D organoid sizes of DIF+ and DIF- HOFs, and mRNA expressions of adipogenesis-related genes, ECMs and TIMPs

To further investigate the molecular mechanism in these effects by PGs, under a variety of conditions of DIF- or DIF+ and in the absence or presence of PGs, changes in the sizes of 3D HOFs organoids were compared to the mRNA expression of several factors associated with adipogenesis related genes (*ΠΠΑΡγ* , *LEPTIN* and *Adipo Q*), and ECMs (*COL1, COL4, COL6* and *FN*) (Fig. 4). Among the factors tested, a significant reverse correlation between 3D HOF organoid sizes and the mRNA expression of *COL1* was observed. This reverse correlation was also confirmed by immunostaining for COL1 (Fig. 5). To study this issue further, since the related factors that influence the metabolism of ECMs including COL1, the mRNA expression of ECM regulatory genes (*LOX* and *EPAS1*) and tissue inhibitors of metalloproteinases 1-4 (*TIMPs 1-4*) were examined (Fig. 6). Interestingly, among these, fluctuations in the mRNA expressions of*LOX* and *TIMP2* under several conditions also strongly corresponded with those of *COL1* , as shown in Fig. 4. Furthermore, the expression of TIMPs 1 and 4 were modulated upon adipogenesis, and those of TIMPs 1 and 3 may also be affected by PGs, although those changes were not significantly correlated with the expressions of COL1, LOX and TIMP2 mRNA. Taken together, adipogenic differentiation and PGs greatly affected the sizes of the 3D HOF organoids, in which COL1, LOX and TIMP2 were recognized as key underlying factors.

3.5 | Ultrastructure and physical properties of the 3D organoid of DIF+ and DIF- HOFs in the absence and presence of PGs.

We next examined the ultrastructure of organoids by electron microscopy (EM) and their physical properties by means of a micro-squeezer analysis of the HOF organoid under several conditions, as described above. Upon adipogenic differentiation, EM showed that the sizes of the 3D HOF organoids were again significantly

greater and this was markedly suppressed in the presence of PGs. Furthermore, ECM deposits observed on the surfaces of 3D HOF organoids of both DIF- and DIF+ were significantly increased in the presence of PGs (panel A). Concerning the physical properties determined by a micro-squeezer, significantly higher mechanical indentation forces were required for organoids in the presence of PGs, and those PGs-induced effects were further enhanced upon adipogenic differentiation (panel B).

4 | DISCUSSION

Different incidents of DUES were reported among the PGs clinically used as anti-glaucoma medications; 60.0% in patients using BIM, 50.0% in those using travoprost, 24.0% in those using LAT, and 18.0% in those using tafluprost (Inoue, Shiokawa, Wakakura & Tomita, 2013). Miki et al. reported that DUES was observed before trabeculectomy procedures in 18 of 74 eyes (24.3%) in patients that has been treated with BIM (50.0%), LAT (16.7%), tafluprost (5.5%) and travoprost (27.8%) (Miki et al., 2017). Furthermore, they also reported that no significant recurrent IOP elevation at 24-month post-trabeculectomy was found ($P < 0.001$) smaller in patients using BIM (31.3%) than LAT (83.2%), tafluprost (45.5%), or travoprost (65.6%). Based upon these observations, they suggested that BIM may cause an unfavorable post-trabeculectomy outcome in addition to inducing a high incidence of DUES. In the current study of the concentration dependency of PGs using 3D HOF organoids, we also demonstrated the most potent efficacy of BIM-A among PGs in the suppression of the adipogenesis (DIF+) induced enlargement in the 3D HOF organoids.

BIM-A is an acid form of prost-type PG analogues derived from PGF2α by the addition of a phenyl base at C-17 that is important for binding to the prostanoid FP receptor, and conservation of the C-15 hydroxyl base (Taketani, Yamagishi, Fujishiro, Igarashi, Sakata & Aihara, 2014). BIM-A binds directly to a dimer prostamide receptor, which is composed of the FP receptor and an FP receptor splice variant (Liang et al., 2008). This suggests that BIM-A induced DUES may reasonably be related to FP receptors. In fact, Taketani et al. recently reported that prostamide PG analogues induced the inhibition of the adipogenesis through stimulation of the FP receptor using 2D cultured 3T3-L1 cells and FP receptor knockout mice (Taketani, Yamagishi, Fujishiro, Igarashi, Sakata & Aihara, 2014). It was revealed that functionally active FP receptors are located on human trabecular meshwork (TM) cells (Sharif, Kelly & Crider, 2003), and thus FP receptor PG agonists could affect TM outflow of the aqueous humor (Lim et al., 2008; Toris, Zhan & Camras, 2004). Taken together with the effects of PGs on trabeculectomy outcomes, as suggested above, PGs may affect mechanisms other than adipogenesis, such as ECM metabolism, even in adipocyte tissues. Our recent pilot studies demonstrated that PGs significantly suppressed the 3D organoid maturation of 3T3-L1 cells or HOFs in which their adipogenesis and /or ECM expressions were presumably altered (Ida, Hikage, Itoh, Ida & Ohguro, 2020; Itoh, Hikage, Ida & Ohguro, 2020). Thus, we concluded that this *ex vivo* model using a 3D culture of 3T3-L1 cells or HOFs could replicate DUES, and thus would be a useful strategy for understanding their molecular pathology.

Compared to conventional 2D cell cultures, the 3D organoid culture method is more beneficial for studies of the structure of tissues in a closed biological environment including the network of ECM proteins (Chun, Hotary, Sabeh, Saltiel, Allen & Weiss, 2006). In the present study, we report that the efficacy of adipogenic induction toward HOFs was much higher in 3D organoid cultures than in conventional 2D cell cultures. In terms of this difference between 2D and 3D cell cultures, we speculated that adipogenesis may prefer a 3D environment. In fact, Miyamoto et al. also reported a much higher efficacy of adipogenic induction of the human adipose-derived stem cells in 3D cell cultures than in 2D cell cultures (Miyamoto, Ikeuchi, Noguchi, Yagi & Hayashi, 2017). Furthermore, our group recently found that HIF2A is pivotally involved in mediating LOX-dependent ECM accumulation, resulting in a significant enhancement in the levels of orbital fat in patients with thyroid associated orbitopathy (TAO) in a study using 3D organoid cultures, although these HIF2A effects were not observed in conventional 2D cell cultures (Hikage, Atkins, Kahana, Smith & Chun, 2019).

It is well known that ECM provides not only structural support to organs, but also functions to modify and regulate cell-cell signals as well as various other cellular functions (Perumal, Antipova & Orgel, 2008). Among ECM, collagens (COLs), triple helical proteins, are located at the cell-ECM interface, and among

more than 30 COLs and COL-related proteins, the most abundant is COL1 (Ricard-Blum, 2011). Among other major COLs, COL4 is a main COL of the basement membrane ECM which surrounds each adipocyte (Aratani & Kitagawa, 1988; Mak & Mei, 2017). COL6 forms microfibrils at the interface between the basement membrane and thick bundles of COL1, and is involved in important functions of several tissues to support maintaining the stemness and differentiation of many cells, including the adipogenesis of adipocytes (Liu et al., 2017). FN is a widely distributed glycoprotein which defines cell shape and contractility and is closely associated with COL1 (Sottile & Hocking, 2002; Spiegelman & Ginty, 1983). In adipocytes or adipose tissues, it is known that the expressions of COL1, COL4, COL6 and FN are altered during adipogenesis, and therefore are pivotally involved in their adipogenesis (Kim, Choi, Yim & Lee, 2013; Nakajima, Muroya, Tanabe & Chikuni, 2002). Previous studies using 2D cultures of 3T3-L1 preadipocytes demonstrated that *in vitro* remodeling is associated with the alteration of COL1 and FN rich ECM in undifferentiated cells into basal membrane type-rich ECM such as COL4, in differentiated cells (Aratani & Kitagawa, 1988). In fact, in previous studies using conventional 2D cultures of 3T3-L1 cells, we confirmed that, the downregulation of COL1 and FN and the up-regulation of COL4 and COL6 expression occurs using 3D organoids of HOFs or 3T3-L1 cells (Ida, Hikage, Itoh, Ida & Ohguro, 2020; Itoh, Hikage, Ida & Ohguro, 2020). In the present study, these adipogenesis induced alterations were reproduced, as shown in Fig. 4. Concerning the effects of PGs toward 3D HOFs organoids with adipogenesis (DIF+), the upregulation of COL1 and the downregulation of COL6 and FN mRNA expressions were again observed (Fig. 4). However, in 3D HOF preadipocyte organoids (DIF-), only the upregulation of COL1 mRNA expression was recognized. These collective data indicate that downregulation by adipogenesis, or upregulation by PGs of COL1 occurred independently, while the mRNA expression of COL4, COL6 and FN were modulated by PGs in conjunction with adipogenesis. Interestingly, in our previous study using organoids of 3T3-L1 cells, in which adipogenic differentiation is more potent as compared to the HOFs, the effects of PGs on COL1 mRNA expression of 3D organoids with adipogenesis (DIF+) were identical with those of HOFs, while alterations of other three ECMs by PGs were different from those of HOFs (Ida, Hikage, Itoh, Ida & Ohguro, 2020; Itoh, Hikage, Ida & Ohguro, 2020). Structurally, adipocytes are known to be surrounded by a number of ECMs constituting interstitial fibers and pericellular basement membranes (Chun, Hotary, Sabeh, Saltiel, Allen & Weiss, 2006; Lijnen, Maquoi, Demeulemeester, Van Hoef & Collen, 2002). In the present study, these ECM networks were abundantly visualized by EM (Fig. 6A). In addition, adipogenesis induced the formation of more abundant and packed ECM deposits on the surface of the 3D HOFs organoids, and the levels of these deposits were further enhanced in the presence of PGs. Furthermore, based on these enhancements of ECMs, in which COL1 was largely involved, the physical solidity of the 3D HOFs organoids were significantly increased. Such COL1 induced enhancement of fibrosis was also reported in a murine bleomycin-induced pulmonary fibrosis model induced by an FP agonist (Aihara et al., 2013; Oga et al., 2009; Olman, 2009).

The synthesis of COL1 is known to be a complex process, and includes a series of post-translational modifications (Chun, 2012). Among these, intra- and extra-cellular post-translational modifications of specific lysine residues mediated by LOX are pivotal in forming covalent COL cross-linking for fibrillogenesis and the stability of fibrils (McKay, Priyadarsini & Karamichos, 2019). These maturation processes of COL cross-linkages varies from tissue to tissue, and are most likely related to the physiological states of different tissues (Wei, Gao, Wu, Qin & Yuan, 2020). LOX and four LOX-like proteins are members of copper-containing amine oxidases, and functionally oxidize lysine and hydroxylysine residues of ECMs, such as COLs and elastin, as well as other soluble substrates (Barker, Cox & Erler, 2012; Smith-Mungo & Kagan, 1998). The LOX precursor is secreted mainly by smooth muscle cells and fibroblasts, and is then hydrolyzed into the catalytically active mature form of LOX and a catalytically inactive peptide(Lucero & Kagan, 2006; Papadantonakis, Matsuura & Ravid, 2012). This activated LOX functions to form crosslinks between COL1, elastin and others through their lysine residues, which is subsequently transformed into their non-soluble states (López, González, Hermida, Valencia, de Teresa & Díez, 2010). Our group previously found that in addition to LOX, the Endothelial Per-Arnt-Sim domain protein 1 (EPAS1) encoding hypoxia-inducible factor-2A (HIF2A) is also involved in the regulation of the ECM remodeling in orbital adipose tissue fibrosis in TAO (Hikage, Atkins, Kahana, Smith & Chun, 2019). In fact, HIF2A was identified as a pivotal regulator of LOX-induced ECM fibrillogenesis and tissue stiffness (Taddei, Giannoni, Comito & Chiarugi, 2013). However, in the pre-

sent study, the mRNA expression of EPAS1 was not significantly altered upon adipogenesis and/or in cases of PGs. Since our HOFs were obtained from noninflammatory orbital fat tissues, it is possible that they are different from those from patients with TAO. Alternatively, ECMs are mainly produced by fibroblasts and are also degraded by the family of MMP proteins (Chun, 2012). The balance between the production and degradation of ECMs is critically regulated by TIMP, and it is well known that this MMP/TIMP regulatory mechanism contributes to a number of physiological and pathological states (Cui, Hu & Khalil, 2017). In the present study, adipogenesis and/or PGs induced alterations in the sizes of the 3D HOFs organoids were exclusively correlated inversely with mRNA expressions of LOX and TIMP2, in addition to COL1. As described above, since it is well known that LOX and TIMP2 are in close contact with COL1 metabolism (Sato & Takino, 2010), it is reasonable to assume that changes in COL1 expression should be further reinforced by the LOX induced enhancement of the COL1 crosslinking and the TIMP2 induced suppression of COL1 degradation. However, the mRNA expression of TIMPs 1 and 3, and TIMP4 were also altered by PGs and adipogenesis, respectively, suggesting that other unknown mechanisms may well be associated with this process. Thus, further investigations related to the roles of MMPs and others will be required.

Author contributions: K.I. designed and performed the experiments, analyzed the data and wrote the paper. Y.I. performed experiments. H.O. analyzed the data and provided conceptual advice. F.H. designed experiments, analyzed the data, and contributed to the writing of the manuscript.

Competing financial interests: Nothing to disclose.

Bullet point summary

What is already known

- PGs induce deepening of the upper eyelid sulcus (DUES) through FP receptor.
- PGs induced effects toward orbital adipocyte metabolism are related to DUES pathology.

What this study adds

- 3D culture of human orbital fibroblasts (HOFs) could well replicate DUES pathogenesis.
- PGs significantly altered ECM expression and physical stiffness of the 3D organoid.
- These effects by PGs closely correlated with their LOX, COL1 and TIMP2 expressions.

Clinical significance

- LOX, COL1 and TIMP2 are pivotally involved in the molecular pathogenesis of DUES.
- Modification of these factors may be applicable as therapeutic strategy of DUES.

ΦΙΓΥΡΕ 1. ἤανγες ιν τηε σιζες οφ 3Δ οργανοιδς οφ ηυμαν ορβιταλ φιβροβλαστς (ΗΟΦς) δυρινγ τηε 3Δ ςελλ ςυλτυρε (Α), ςονφοςαλ ιμμυνοσταινινγ ιμαγες βψ λιπιδ σταινινγ (ΒΟΔΙΠΨ), πηαλλοιδιν, ανδ ΔΑΠΙ οφ 2Δ ανδ 3Δ ςυλτυρεδ ΗΟΦς (Β), ανδ μΡΝΑ εξπρεσσιονς οφ *ΠΠΑΡγ* οφ 2Δ ορ 3Δ ςυλτυρεδ ΗΟΦς (˜).

Panel A: Mean sizes of the 3D organoids of HOFs preadipocytes (DIF-, closed circles) and for adipogenic differentiation (DIF+, closed squares) were plotted during the 12 days period of the 3D culture, and representative phase contrast images are shown. Scale bar: 100 μm. Panel B: At Day 12, 2D cultured HOFs (DIF- or DIF+) or 3D HOFs organoids (DIF- or DIF+) were immunostained with BODIPY (green), Phalloidin (red) and DAPI (blue). Scale bar: 100 μm. Panel C: mRNA expressions of*ΠΠΑΡγ* of 2D or 3D cultured HOFs (DIF- or DIF+) was plotted. All experiments were performed in duplicate using fresh preparations consisting of 5 organoids each. Data are presented as the arithmetic mean ± the standard error of the mean (SEM). ****P <0.001 (ANOVA followed by a Tukey's multiple comparison test).

FIGURE 2. Changes in the sizes of 3D organoids of HOFs during the 3D cell culture in the absence or presence of different concentrations of PGs.

In the presence of 1 (open circles), 100 (open squares) or 10000 nM (open triangles) of Bimatoprost acid (BIM-A), PGF2α or latanoprost acid (LAT-A), changes in the mean sizes of the HOFs organoids of DIF during

the 12 day period of the culture were plotted (left panels), and their mean sizes at Day 12 were compared among the different concentrations (right panels). All experiments were performed in triplicate using fresh preparations consisting of 16 organoids each. Data are presented as the arithmetic mean ± standard error of the mean (SEM). *P <0.05, *** P <0.005 (ANOVA followed by a Tukey's multiple comparison test).

FIGURE 3. Changes in the sizes of 3D organoids of HOFs preadipocytes during the 3D cell culture in the absence or presence of different concentrations of PGs.

The mean sizes of the organoids of HOFs preadipocytes without (open circles) or with 100 nM Bimatoprost acid (BIM-A, closed squares) or 100 nM PGF2α (closed triangles) were measured at Day 1, 2, 3 or 12, and compared among the treatment groups. All experiments were performed in triplicate using fresh preparations consisting of 16 organoids each. Data are presented as arithmetic means ± standard error of the mean (SEM). **** P <0.001 (ANOVA followed by a Tukey's multiple comparison test).

FIGURE 4. Comparison between the mean sizes of 3D HOFs organoids and their gene expressions of adipogenesis related genes and ECMs among several experimental conditions.

At Day 12, 3D organoids of HOFs preadipocytes (DIF-) and their differentiation (DIF+) in the absence or presence of 100 nM Bimatoprost acid (BIM-A) or 100 nM PGF2α were subjected to qPCR analysis to estimate the mRNA expression of adipogenesis related genes (*ΠΠΑΡγ* ,*LEPTIN* , *Adipo Q*) and ECMs (*COL 1* : collagen 1,*COL 4* : collagen 4, *COL 6* : collagen 6, *FN* : fibronectin). The values were compared with the mean sizes of the 3D HOF organoids among several treatment groups as shown in Figs. 1-3. All experiments were performed in duplicate using fresh preparations consisting of 4 organoids each. Data are presented as the arithmetic mean ± standard error of the mean (SEM). * P <0.05, **P <0.01, *** P <0.005, ****P <0.001 (ANOVA followed by a Tukey's multiple comparison test).

FIGURE 5. Representative confocal immunofluorecein images of the expression of COL 1 in 3D HOF organoids.

At Day 12, 3D culture organoids of HOF preadipocytes (DIF-) and their differentiation (DIF+) in the absence or presence of 100 nM Bimatoprost acid (BIM-A) or 100 nM PGF2α were immunostained with specific antibodies of COL1 (collagen 1, green), DAPI (blue) and phalloidin (red). Scale bar: 100 μm. All experiments were performed in duplicate using fresh preparations consisting of 5 organoids each.

FIGURE 6. mRNA expression of ECM regulatory genes (*LOX*,*EPAS1*), and tissue inhibitors of metalloproteinases (TIMPs) among several experimental conditions.

At Day 12, 3D organoids of 3D HOFs preadipocytes as the control (DIF-) and their differentiation (DIF+) in the absence or presence of 100 nM Bimatoprost acid (BIM-A) or 100 nM PGF2α were subjected to qPCR analysis to estimate the mRNA expression of ECM regulatory genes including*LOX* and *EPAS1* , and tissue inhibitors of metalloproteinases 1-4 *(TIMP 1-4)* . All experiments were performed in duplicate using fresh preparations consisting of 4 organoids each. Data are presented as the arithmetic mean ± standard error of the mean (SEM). *P <0.05, ** P <0.01, ***P <0.005, **** P <0.001 (ANOVA followed by a Tukey's multiple comparison test).

FIGURE 7. Ultrastructure and physical properties of 3D HOFs organoids among several experimental conditions.

Panel A: At Day 12, 3D organoids of HOFs preadipocytes as the control (DIF-) and their differentiation (DIF+) in the absence or presence of 100 nM Bimatoprost acid (BIM-A) or 100 nM PGF2α were subjected to analysis of their ultrastructure by electron microscopy (EM, scale bar: 10 μm). Panel B: Among several experimental conditions as above, physical property by a micro-squeezer analysis was performed using 10 freshly prepared organoids. A single 3D organoid placed on a 3-mm × 3-mm plate was compressed to 50% deformation during 20 sec, those were continuously monitored by a microscopic camera (left panel, S: microsensor of the mechanical force (μN), P: compression plate, Org: single 3D organoid, D: the distance across

3D organoid). Its requiring force was measured, and the force/displacement value (μN/μm) was plotted (right panel). *** P<0.005 (ANOVA followed by a Tukey's multiple comparison test).

References

(2017). European Glaucoma Society Terminology and Guidelines for Glaucoma, 4th Edition - Chapter 3: Treatment principles and options Supported by the EGS Foundation: Part 1: Foreword; Introduction; Glossary; Chapter 3 Treatment principles and options. The British journal of ophthalmology 101**:** 130-195.

Aihara K, Handa T, Oga T, Watanabe K, Tanizawa K, Ikezoe K*, et al.* (2013). Clinical relevance of plasma prostaglandin F2alpha metabolite concentrations in patients with idiopathic pulmonary fibrosis. PLoS One 8**:** e66017.

Aihara M, Shirato S, & Sakata R (2011). Incidence of deepening of the upper eyelid sulcus after switching from latanoprost to bimatoprost. Jpn J Ophthalmol 55**:** 600-604.

Alm A (2014). Latanoprost in the treatment of glaucoma. Clin Ophthalmol 8**:** 1967-1985.

Alm A, Grierson I, & Shields MB (2008). Side effects associated with prostaglandin analog therapy. Survey of ophthalmology 53 Suppl1**:** S93-105.

Aratani Y, & Kitagawa Y (1988). Enhanced synthesis and secretion of type IV collagen and entactin during adipose conversion of 3T3-L1 cells and production of unorthodox laminin complex. J Biol Chem 263**:**16163-16169.

Barker HE, Cox TR, & Erler JT (2012). The rationale for targeting the LOX family in cancer. Nature reviews Cancer 12**:** 540-552.

Chun TH (2012). Peri-adipocyte ECM remodeling in obesity and adipose tissue fibrosis. Adipocyte 1**:** 89-95.

Chun TH, Hotary KB, Sabeh F, Saltiel AR, Allen ED, & Weiss SJ (2006). A pericellular collagenase directs the 3-dimensional development of white adipose tissue. Cell 125**:** 577-591.

Cui N, Hu M, & Khalil RA (2017). Biochemical and Biological Attributes of Matrix Metalloproteinases. Progress in molecular biology and translational science 147**:** 1-73.

Evans RM, Barish GD, & Wang YX (2004). PPARs and the complex journey to obesity. Nat Med 10**:** 355-361.

Gregoire FM, Smas CM, & Sul HS (1998). Understanding adipocyte differentiation. Physiological reviews 78**:** 783-809.

Hikage F, Atkins S, Kahana A, Smith TJ, & Chun TH (2019). HIF2A-LOX Pathway Promotes Fibrotic Tissue Remodeling in Thyroid-Associated Orbitopathy. Endocrinology 160**:** 20-35.

Ida Y, Hikage F, Itoh K, Ida H, & Ohguro H (2020). Prostaglandin F2α agonist-induced suppression of 3T3-L1 cell adipogenesis affects spatial formation of extra-cellular matrix. Sci Rep 10**:** 7958.

Inoue K, Shiokawa M, Wakakura M, & Tomita G (2013). Deepening of the upper eyelid sulcus caused by 5 types of prostaglandin analogs. Journal of glaucoma 22**:** 626-631.

Itoh K, Hikage F, Ida Y, & Ohguro H (2020). Prostaglandin F2α Agonists Negatively Modulate the Size of 3D Organoids from Primary Human Orbital Fibroblasts. Invest Ophthalmol Vis Sci 61**:** 13.

Jayaprakasam A, & Ghazi-Nouri S (2010). Periorbital fat atrophy - an unfamiliar side effect of prostaglandin analogues. Orbit (Amsterdam, Netherlands) 29**:** 357-359.

Kershaw EE, & Flier JS (2004). Adipose tissue as an endocrine organ. J Clin Endocrinol Metab 89**:** 2548-2556.

Kim B, Choi KM, Yim HS, & Lee MG (2013). Ascorbic acid enhances adipogenesis of 3T3-L1 murine preadipocyte through differential expression of collagens. Lipids in health and disease 12**:** 182.

Liang Y, Woodward DF, Guzman VM, Li C, Scott DF, Wang JW*, et al.*(2008). Identification and pharmacological characterization of the prostaglandin FP receptor and FP receptor variant complexes. Br J Pharmacol 154**:** 1079-1093.

Lijnen HR, Maquoi E, Demeulemeester D, Van Hoef B, & Collen D (2002). Modulation of fibrinolytic and gelatinolytic activity during adipose tissue development in a mouse model of nutritionally induced obesity. Thrombosis and haemostasis 88**:** 345-353.

Lim KS, Nau CB, O'Byrne MM, Hodge DO, Toris CB, McLaren JW*, et al.* (2008). Mechanism of action of bimatoprost, latanoprost, and travoprost in healthy subjects. A crossover study. Ophthalmology 115**:** 790-795.e794.

Liu C, Huang K, Li G, Wang P, Liu C, Guo C*, et al.* (2017). Ascorbic acid promotes 3T3-L1 cells adipogenesis by attenuating ERK signaling to upregulate the collagen VI. Nutrition & metabolism 14**:** 79.

López B, González A, Hermida N, Valencia F, de Teresa E, & Díez J (2010). Role of lysyl oxidase in myocardial fibrosis: from basic science to clinical aspects. American journal of physiology Heart and circulatory physiology 299**:** H1-9.

Lucero HA, & Kagan HM (2006). Lysyl oxidase: an oxidative enzyme and effector of cell function. Cellular and molecular life sciences : CMLS 63**:** 2304-2316.

Mak KM, & Mei R (2017). Basement Membrane Type IV Collagen and Laminin: An Overview of Their Biology and Value as Fibrosis Biomarkers of Liver Disease. Anatomical record (Hoboken, NJ : 2007) 300**:** 1371-1390.

Maruyama K, Tsuchisaka A, Sakamoto J, Shirato S, & Goto H (2013). Incidence of deepening of upper eyelid sulcus after topical use of tafluprost ophthalmic solution in Japanese patients. Clin Ophthalmol 7**:** 1441-1446.

McKay TB, Priyadarsini S, & Karamichos D (2019). Mechanisms of Collagen Crosslinking in Diabetes and Keratoconus. Cells 8.

Miki T, Naito T, Fujiwara M, Araki R, Kiyoi R, Shiode Y*, et al.*(2017). Effects of pre-surgical administration of prostaglandin analogs on the outcome of trabeculectomy. PLoS One 12**:** e0181550.

Miyamoto Y, Ikeuchi M, Noguchi H, Yagi T, & Hayashi S (2017). Enhanced Adipogenic Differentiation of Human Adipose-Derived Stem Cells in an In Vitro Microenvironment: The Preparation of Adipose-Like Microtissues Using a Three-Dimensional Culture. Cell medicine 9**:** 35-44.

Mori S, Kiuchi S, Ouchi A, Hase T, & Murase T (2014). Characteristic expression of extracellular matrix in subcutaneous adipose tissue development and adipogenesis; comparison with visceral adipose tissue. International journal of biological sciences 10**:** 825-833.

Nakajima I, Muroya S, Tanabe R, & Chikuni K (2002). Extracellular matrix development during differentiation into adipocytes with a unique increase in type V and VI collagen. Biology of the cell 94**:**197-203.

Nakakura S, Terao E, Nagatomi N, Matsuo N, Shimizu Y, Tabuchi H*, et al.* (2014). Cross-sectional study of the association between a deepening of the upper eyelid sulcus-like appearance and wide-open eyes. PLoS One 9**:** e96249.

Oga T, Matsuoka T, Yao C, Nonomura K, Kitaoka S, Sakata D*, et al.*(2009). Prostaglandin F(2alpha) receptor signaling facilitates bleomycin-induced pulmonary fibrosis independently of transforming growth factor-beta. Nat Med 15**:** 1426-1430.

Olman MA (2009). Beyond TGF-beta: a prostaglandin promotes fibrosis. Nat Med 15**:** 1360-1361.

Ota T, Aihara M, Narumiya S, & Araie M (2005). The effects of prostaglandin analogues on IOP in prostanoid FP-receptor-deficient mice. Invest Ophthalmol Vis Sci 46**:** 4159-4163.

Papadantonakis N, Matsuura S, & Ravid K (2012). Megakaryocyte pathology and bone marrow fibrosis: the lysyl oxidase connection. Blood 120**:** 1774-1781.

Peplinski LS, & Albiani Smith K (2004). Deepening of lid sulcus from topical bimatoprost therapy. Optometry and vision science : official publication of the American Academy of Optometry 81**:** 574-577.

Perumal S, Antipova O, & Orgel JP (2008). Collagen fibril architecture, domain organization, and triple-helical conformation govern its proteolysis. Proceedings of the National Academy of Sciences of the United States of America 105**:** 2824-2829.

Ricard-Blum S (2011). The collagen family. Cold Spring Harbor perspectives in biology 3**:** a004978.

Sakata R, Shirato S, Miyata K, & Aihara M (2014). Incidence of deepening of the upper eyelid sulcus in prostaglandin-associated periorbitopathy with a latanoprost ophthalmic solution. Eye (Lond) 28**:** 1446-1451.

Sato H, & Takino T (2010). Coordinate action of membrane-type matrix metalloproteinase-1 (MT1-MMP) and MMP-2 enhances pericellular proteolysis and invasion. Cancer science 101**:** 843-847.

Shah M, Lee G, Lefebvre DR, Kronberg B, Loomis S, Brauner SC*, et al.* (2013). A cross-sectional survey of the association between bilateral topical prostaglandin analogue use and ocular adnexal features. PLoS One 8**:** e61638.

Sharif NA, Kelly CR, & Crider JY (2003). Human trabecular meshwork cell responses induced by bimatoprost, travoprost, unoprostone, and other FP prostaglandin receptor agonist analogues. Invest Ophthalmol Vis Sci 44**:** 715-721.

Smith-Mungo LI, & Kagan HM (1998). Lysyl oxidase: properties, regulation and multiple functions in biology. Matrix biology : journal of the International Society for Matrix Biology 16**:** 387-398.

Sottile J, & Hocking DC (2002). Fibronectin polymerization regulates the composition and stability of extracellular matrix fibrils and cell-matrix adhesions. Molecular biology of the cell 13**:**3546-3559.

Spiegelman BM, & Ginty CA (1983). Fibronectin modulation of cell shape and lipogenic gene expression in 3T3-adipocytes. Cell 35**:**657-666.

Taddei ML, Giannoni E, Comito G, & Chiarugi P (2013). Microenvironment and tumor cell plasticity: an easy way out. Cancer letters 341**:**80-96.

Taketani Y, Yamagishi R, Fujishiro T, Igarashi M, Sakata R, & Aihara M (2014). Activation of the prostanoid FP receptor inhibits adipogenesis leading to deepening of the upper eyelid sulcus in prostaglandin-associated periorbitopathy. Invest Ophthalmol Vis Sci 55**:** 1269-1276.

Toris CB, Zhan G, & Camras CB (2004). Increase in outflow facility with unoprostone treatment in ocular hypertensive patients. Archives of ophthalmology (Chicago, Ill : 1960) 122**:** 1782-1787.

Wei S, Gao L, Wu C, Qin F, & Yuan J (2020). Role of the lysyl oxidase family in organ development (Review). Experimental and therapeutic medicine 20**:** 163-172.

Yu C, Kornmuller A, Brown C, Hoare T, & Flynn LE (2017). Decellularized adipose tissue microcarriers as a dynamic culture platform for human adipose-derived stem/stromal cell expansion. Biomaterials 120**:**66-80.

Hosted file

`Figure-1.pdf` available at https://authorea.com/users/353204/articles/477227-enhancement-of-collagen-1-expression-by-prostaglandin-f2%CE%B1-agonists-is-pivotally-involved-in-the-pathogenesis-of-deepening-of-the-upper-eyelid-sulcus

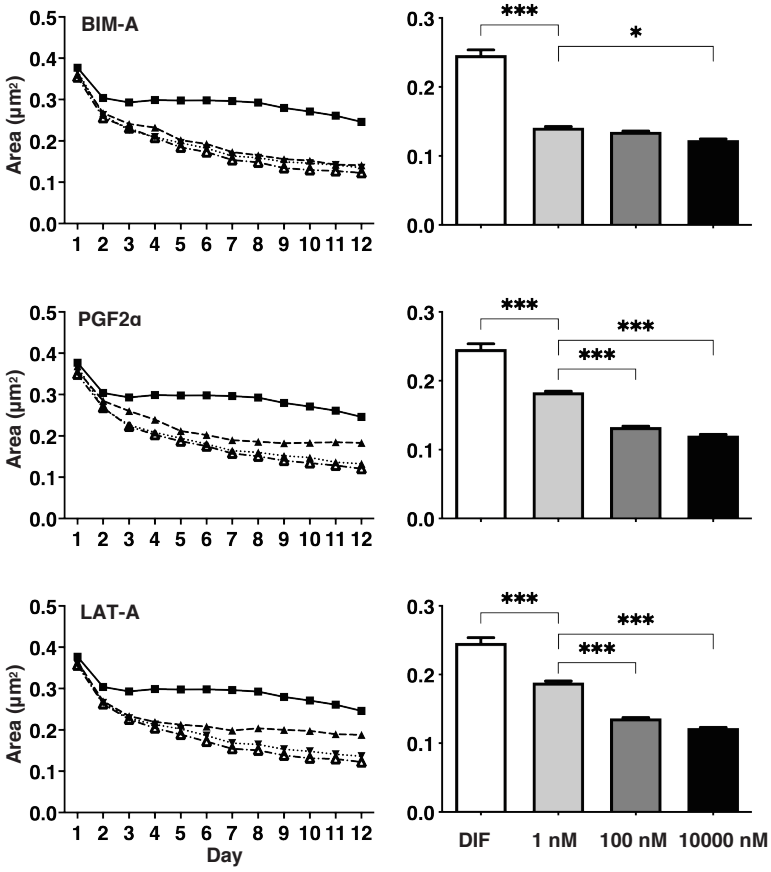

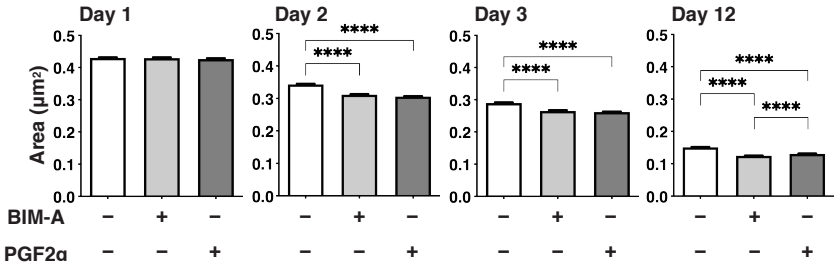

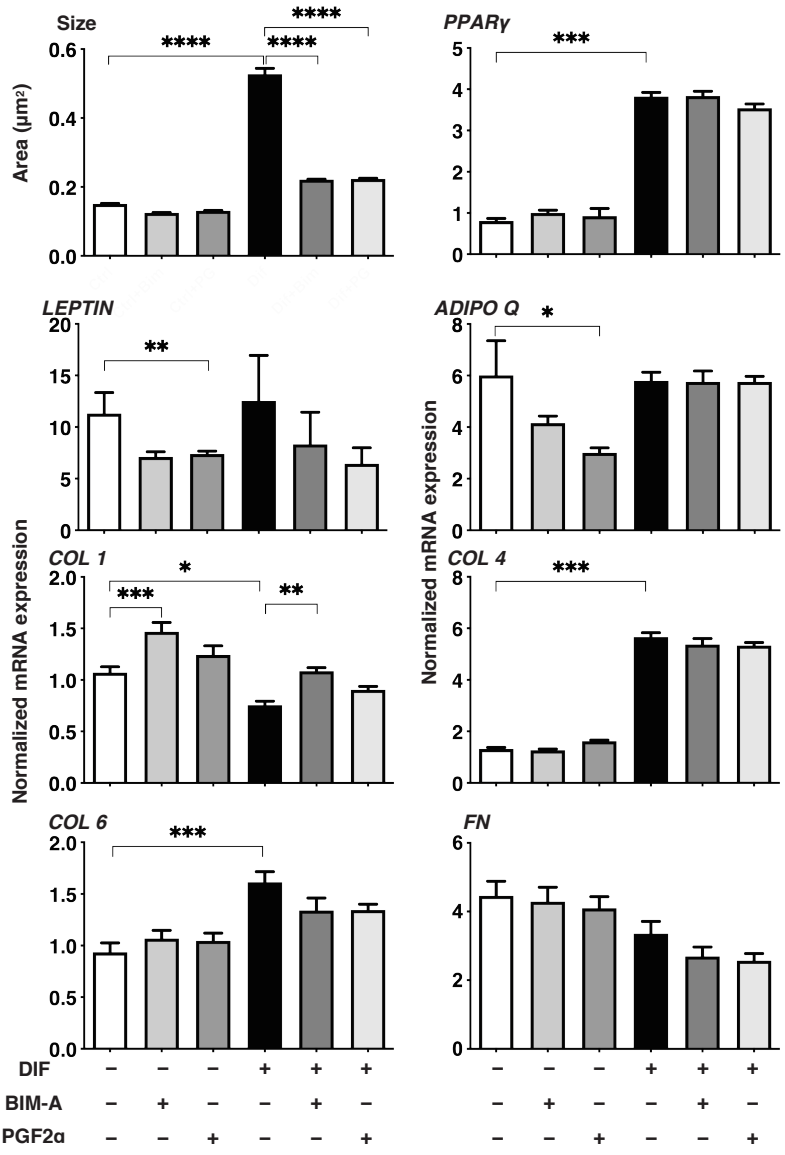

Hosted file

Figure-5.pdf available at https://authorea.com/users/353204/articles/477227-enhancement-of-collagen-1-expression-by-prostaglandin-f2%CE%B1-agonists-is-pivotally-involved-in-the-pathogenesis-of-deepening-of-the-upper-eyelid-sulcus

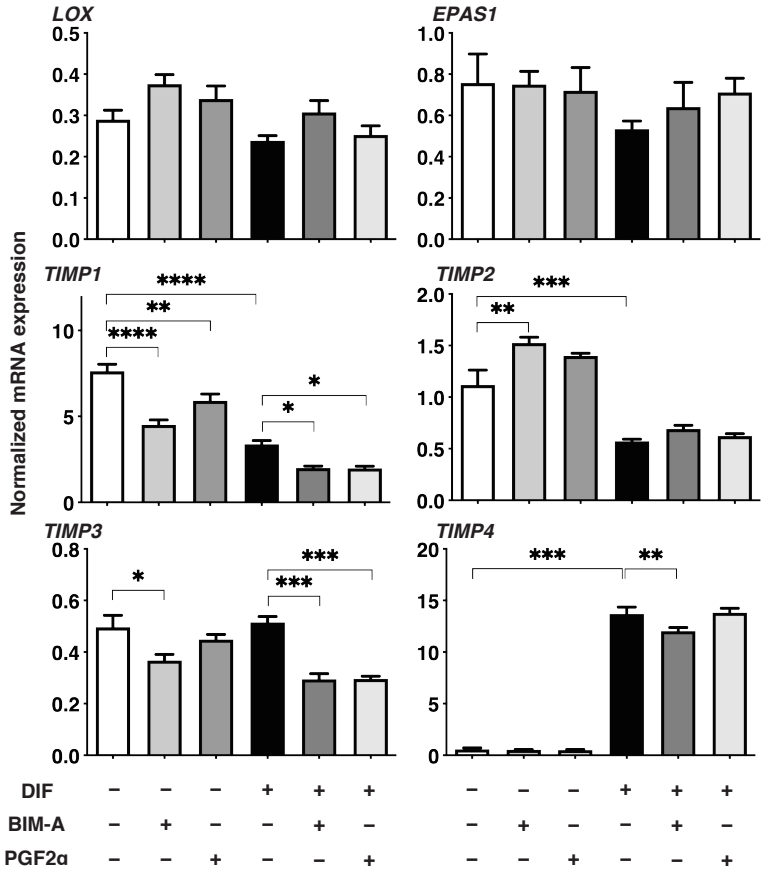

Hosted file

Figure-7.pdf available at https://authorea.com/users/353204/articles/477227-enhancement-of-collagen-1-expression-by-prostaglandin-f2%CE%B1-agonists-is-pivotally-involved-in-the-pathogenesis-of-deepening-of-the-upper-eyelid-sulcus